Water Practice & Technology

IWA PUBLISHING

Water Practice & Technology Vol 19 No 1, 228 doi: 10.2166/wpt.2023.224

Sunflower seed pulp ash as an efficient and eco-friendly adsorbent for Congo red uptake: characteristics, kinetics, and optimization

Majid Mohadesi, Ashkan Gouran, Farzaneh Darabi and Mohsen Samimi *

Department of Chemical Engineering, Faculty of Engineering, Kermanshah University of Technology, Kermanshah, Iran
*Corresponding author. E-mail: m.samimi@kut.ac.ir

MS, 0000-0003-3098-7283

ABSTRACT

This investigation focused on the Congo red uptake, as the azo dye, from an aqueous environment. Herein, ash derived from sunflower seed pulp waste (SSPA) was used as an eco-friendly low-cost adsorbent. Based on the BET results, the specific active surface area of SSPA was approximately 102 m^2/g. The effect of the initial analyte concentration (10–50 mg/L), the concentration of the adsorbent (1–5 g/L), and the processing time (10–240 min) on the rate of Congo red uptake was also evaluated and optimized. According to the results, the maximum dye removal from synthetic solution (91.89%) was achieved at a dye concentration of 50 mg/L, an adsorbent concentration of 3 g/L, and a processing time of 180 min. The maximum SSPA capacity for Congo red uptake from aquatic solution was 15.34 mg/g, achieving under optimized operational conditions. The adsorption process of SSPA also follows a pseudo-second-order kinetic model ($q_e = 15.85$ mg/g; $R^2 > 0.99$), considering the results of BET and FTIR, suggesting that the rate-controlling step in analyte removal is the chemical interaction between functional groups in SSPA and used dye. Finally, the SSPA washing with different solvents showed that the adsorbent treated with 1 M sodium hydroxide still performed well after his five reuses.

Key words: adsorption, ash, Congo red dye, kinetic modeling, sunflower seed pulp

HIGHLIGHTS

- Sunflower seed pulp ash (SSPA) was prepared and applied as an eco-friendly low-cost adsorbent for Congo red uptake.
- Experiments showed the rate-controlling step in dye adsorption is the chemical interaction of functional groups between SSPA and Congo red.
- According to the washing process of the adsorbent used by different solvents, one molar solution had a high capacity to wash the SSPA.

GRAPHICAL ABSTRACT

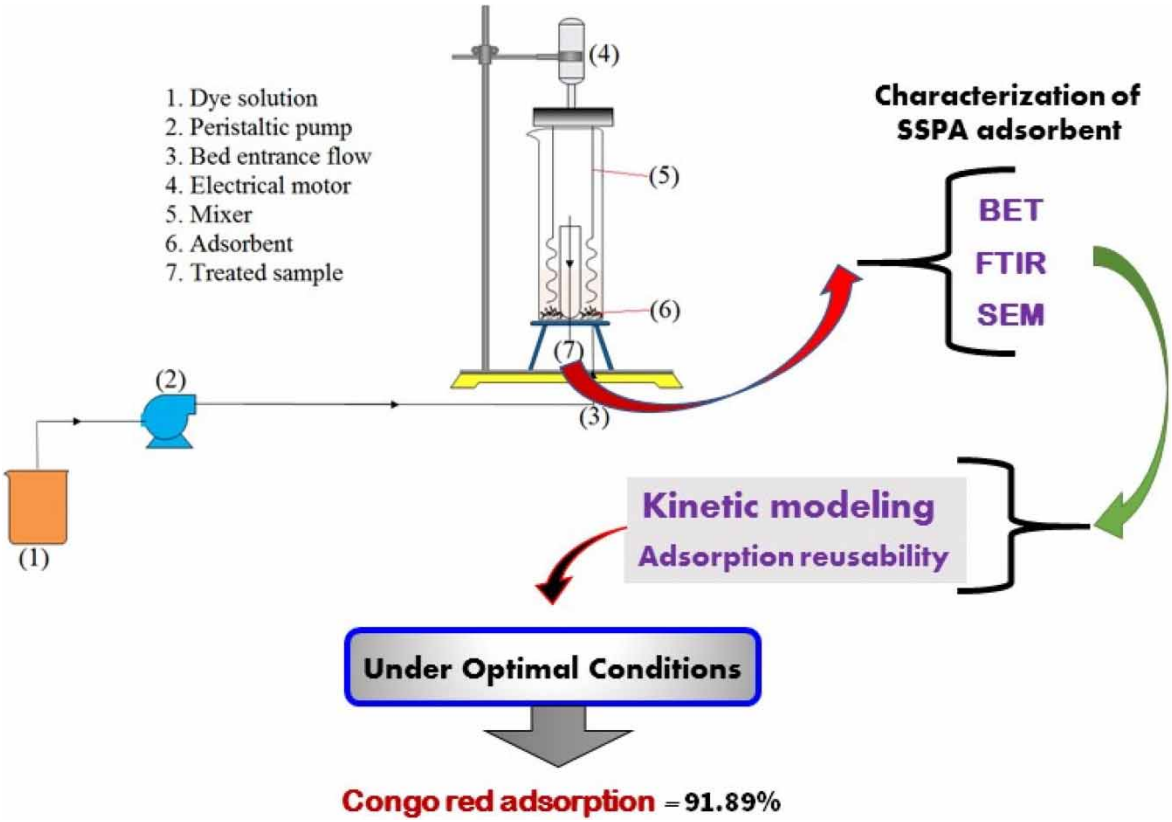

1. INTRODUCTION

There are limited resources of freshwater on earth, and the development of industry and urbanization is leading to the release of large amounts of dyes, pollutants, organic pollutants, and heavy metal ions into natural water resources (Drobyazko *et al.* 2021; Moghadam & Samimi 2022). Azo dyes are principal contaminants produced by industries, such as textile printing, cosmetics, textiles, and food dyes (Oliver Paul Nayagam & Prasanna 2023). Due to the toxicity and high level of non-biodegradability in the environment, dyes are dangerous to the lives of aquatic animals and humans, even in low concentrations (You *et al.* 2018; Samimi & Safari 2022). Polluted water released by industry contains highly carcinogenic and non-biodegradable dyes of Congo red. Wastewater containing Congo red dye is produced in the textile, printing, dyeing, paper, and plastic industries (Hamad & Saied 2021; Khan *et al.* 2022). To reuse these polluted waters, many new and effective adsorbents have been used to remove the contaminants (Mohammadi *et al.* 2021; Nuryadin & Imai 2021; Samimi 2024). Dye-contaminated water is decolorized by conventional methods such as coagulation (Zhou *et al.* 2017; Nimesha *et al.* 2022), photocatalysis (Magdalane *et al.* 2021; Mambwe *et al.* 2021), environmental bacteria (Manjarrez Paba *et al.* 2021), and adsorption (Samimi & Moeini 2020). Among these, the adsorption method is very effective and efficient because it has features, such as low cost, availability of various adsorbents, simplicity of the process, high efficiency, and ease of implementation (Samimi & Shahriari-Moghadam 2023). The adsorption method has been used in many studies to remove Congo red from wastewater. In some studies, different adsorbents such as composite layers made of melamine-formaldehyde and polyvinyl alcohol (Bhat *et al.* 2020), activated carbon nanocomposite made of Guar gum (Gupta *et al.* 2020), pineapple skin (Dai *et al.* 2020), synthetic $Fe_xCo_{3-x}O_4$ nanoparticles (Liu *et al.* 2019), synthesized zeolite and ZnO particles (Madan *et al.* 2019), chitosan/bentonite composite (Abukhadra *et al.* 2019), and NiO–SiO_2 composite particles (Lei *et al.* 2016), were used for the removal of Congo red from wastewater.

The various biosorbents have attracted the attention of researchers due to their cost-effectiveness and acceptable performance in removing Congo red from aqueous solutions containing this type of dye (Siddiqui *et al.* 2023). Among these, it can mention the paper and algae waste collected from bio-related companies (Fawzy & Gomaa

2020), hydroxyapatite nanoparticles synthesized from eggshells (Vinayagam *et al.* 2023), hydroxyapatite nanorods adsorbents synthesized from phosphogypsum wastes (Bensalah *et al.* 2020), magnetically lignin-based bioadsorbent (Zong *et al.* 2023), dried powdered cabbage waste (Wekoye *et al.* 2020), Jojoba seed wastes (Al-Zoubi *et al.* 2020), carbon from leaves and stem of water hyacinth (Extross *et al.* 2023), sugarcane bagasse prepared with tartaric acid (Said *et al.* 2020), activated carbon from ashitaba waste and walnut shells (Li *et al.* 2020), saffron stem shells (Dbik *et al.* 2020), eucalyptus leaf powder (Kumari *et al.* 2020), and natural and modified Clinoptilolite with a surfactant (Nodehi *et al.* 2020).

In some previous studies, synthetic adsorbents, which have a high price and are harmful to the environment, or cheap adsorbents, whose surface modifications require using chemical materials, which are dangerous to nature and microorganisms, have been used. Many studies have been carried out on using sunflower derivatives for adsorption, such as sunflower head and stem as adsorbents to remove heavy metals from aqueous media (Mohmmadkhani *et al.* 2016) and sunflower stalks to remove lead and cadmium from aqueous solution (Jalali & Aboulghazi 2013). This work aimed to use an inexpensive and eco-friendly adsorbent produced during a simple process to remove colored wastewater. Sunflower seed pulp ash (SSPA) was used as an adsorbent to remove Congo red dye from aqueous solutions in a continuous fluidized bed reactor. The effects of operational variables on Congo red uptake, such as initial dye concentration, process time, and SSPA amount, were also studied.

2. MATERIALS AND METHODS

2.1. Materials

Using Congo red dye (Merck, high purity), synthetic solutions were prepared and used in this study as feed. The sunflower seed pulp was obtained from local shops producing sunflower oil (Kermanshah, Iran). Ethanol (Merck, 99.8%) and sodium hydroxide (NaOH) (Merck, ACS reagent, ≥97.0%, pellets) were used in the adsorbent washing step. All experiments used double-distilled water.

2.2. Preparation of adsorbent

The ash powder used in the present study was prepared from sunflower seed pulp as agricultural waste. First, the prepared sunflower seed pulp was put into the furnace and the temperature was increased to 600 °C at a rate of 5 °C/min, held at this temperature for 1 h, and then was cooled to ambient temperature. The resulting material, SSPA, was crushed and grinded, and the particles smaller than 45 μm were separated for testing. Finally, the prepared powder particles were stored in an insulated container. Before the experiments, no chemical operations or physical treatment were conducted on ash obtained from sunflower seed pulp.

2.3. Methods

The scheme of the setup prepared for all experiments is shown in Figure 1. In this study, Congo red dye removal was investigated using the adsorption process in a fluidized bed reactor (the volume of the reactor is 100 mL). The fluidized bed reactor was specifically customized to investigate the adsorption of various pollutants. It has not only the same characteristics as a fluidized bed but also being able to establish proper mixing to increase the contact between the adsorbent surface and pollutant molecules. The feed containing the dye solution made with a desired concentration and specific amounts of ash made of sunflower seed pulp was tested at different contact times in the mentioned fluidized bed reactor. The feed solution in a container was pumped using a peristaltic pump (BT100-1F model) into the reactor from the bottom, leading to the adsorbent fluidization.

To increase the efficiency of mixing and adsorption, the laboratory setup used an electrical motor with a speed of 600 rpm to rotate two mechanical stirrers. After a specified period, after centrifugation (to separate the adsorbent from the treated wastewater), the sample was removed from the setup and discarded as the final treated sample. Congo red dye concentration was measured using a UV-Vis spectrophotometer (PG Instruments, UK, Model: T80 + +) at 497 nm with a calibration curve. Device calibration curves were generated individually by preparing solutions with different dye concentrations. The variables studied included initial dye concentration, process time, and amount of adsorbent. The SSPA capacity in dye uptake and Congo red removal percentage

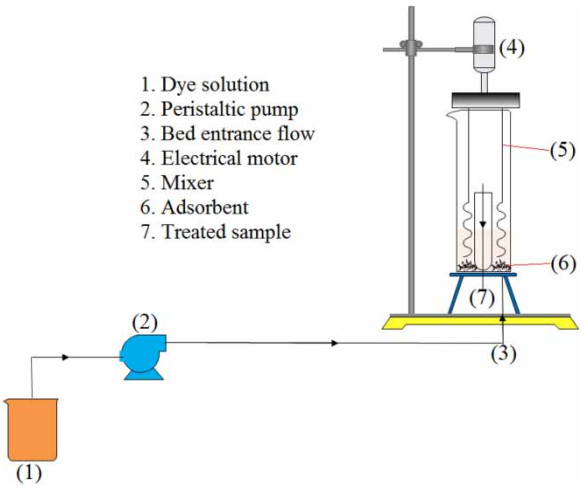

Figure 1 | Schematic of the setup used in this study to remove Congo red dye by SSPA.

were determined as follows (Samimi & Nouri 2023):

$$\text{Congo red removal } \% = \frac{C_i - C_t}{C_i} \times 100 \tag{1}$$

$$q_t = \frac{C_i - C_t}{M} \tag{2}$$

where C_i is the concentration of initial dye in mg/L, C_t is the concentration of dye at residence time t in mg/L, q_t (mg/g) is the SSPA capacity in Congo red removal at residence time t, and M (g/L) is the SSPA amount in dye solution.

2.4. Characterization of SSPA

FTIR spectroscopy was applied to identify the functional groups of the SSPA adsorbent. The surface morphology and specific surface area, as well as the surface particle size, were evaluated through SEM and BET analysis (N_2 gas adsorption at 77 K), respectively.

2.5. Adsorbent washing with solvents

To wash ash derived from sunflower seed pulp, ethanol, one molar of NaOH, and double-distilled water at 65 °C were used and the results were compared. Accordingly, the sunflower seed pulp collected from the experiment was stirred with 100 mL of each solvent (ethanol, NaOH solution, and double-distilled water) for 180 min and after filtration using a filter paper and drying at ambient temperature for 12 h, it was used again.

3. RESULTS AND DISCUSSION

3.1. Characterization of SSPA adsorbent

The BET results of SSPA showed a total pore volume of 0.0990 cm^3/g, a specific surface area of 102.68 m^2/g, and a mean pore diameter of 3.859 nm. The specific surface area results of SSPA with other similar adsorbents are presented in Table 1. The SEM image of SSPA is also shown in Figure 2.

Table 1 | Comparison of BET results of the used adsorbent in this work with other studies

Adsorbent	Specific surface area (m^2/g)	Reference
Natural clinoptilolite	11.93	Nodehi *et al.* (2020)
Activated carbon prepared from sunflower seed hull	21.06	Thinakaran *et al.* (2008)
Sunflower waste – manganese iron oxide composite	47.14	Uygunoz *et al.* (2022)
Fly ash from a local power plant	7.53	Harja *et al.* (2022)
SSPA	102.68	This study

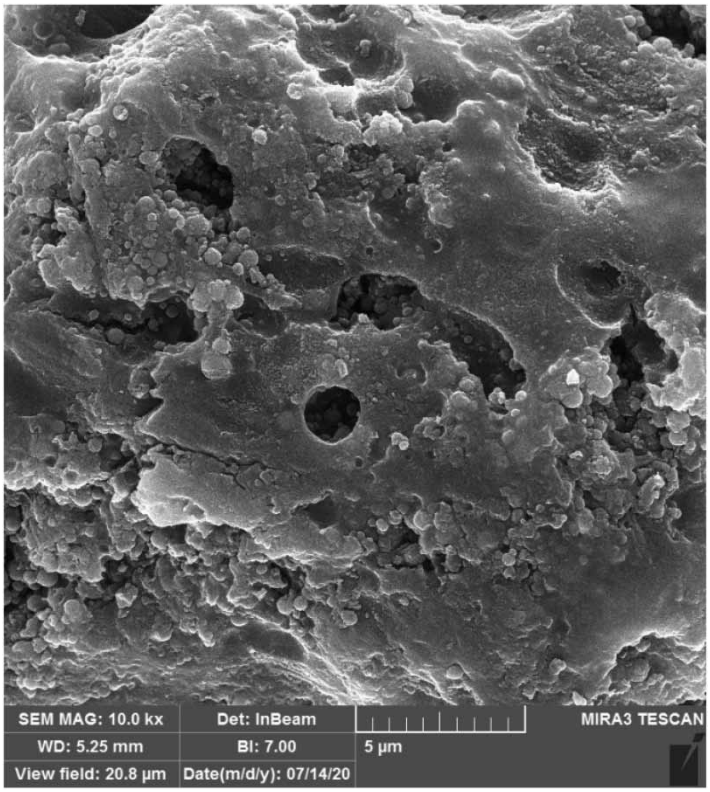

Figure 2 | SEM image of SSPA.

FTIR spectroscopy is an essential technique to characterize functional groups and the variation study of these groups in the adsorbent (Ehzari *et al.* 2022). The FTIR spectra of the ash adsorbent before and after Congo red adsorption are shown in Figure 3(a) and 3(b), respectively. The bonds of 3,422.58 and 3,502.9 cm^{-1} are attributed to the tensile frequency of the OH at the SSPA surface. The adsorption peak of 2,856.99 and 2,923.47 cm^{-1} is related to the symmetric tensile frequency of the $-CH_3$ group. The peak of 1,627.66 cm^{-1} shows the tensile frequency of C = O bond in carboxylic acid, which is bonded with intramolecular hydrogen (Han *et al.* 2010). The peak of 1,387.86 cm^{-1} is caused by the symmetric curvature of $-CH_3$. The presence of an adsorption peak at 1,084.54 cm^{-1} may be related to the frequency change at OH and the tensile frequency at C–O–C in the cellulosic structure of the adsorbent. The FTIR results showed that the surface of the adsorbent is abundant with different oxygen functionalities (O–H, C = O, C–O–C). These functionalities will act as active binding sites for the effective uptake of anionic dyes from the water phase (Al-Zoubi *et al.* 2020). As shown in Figure 3(b), after the adsorption of Congo red, the peak of tensile frequencies of OH as well as the tensile frequency of C = O in carboxylic acid with bounded intramolecular hydrogen changed, and frequencies of 3,502.90 and 1,627.66 cm^{-1}, respectively, reduced to 3,426.20 and 1,625.33 cm^{-1}.

3.2. Effect of operational variables on the elimination of Congo red

In this study, the effects of different variables such as initial concentration of Congo red, adsorbent concentration, and process time on Congo red dye removal were evaluated. The values of each of these variables along with their dimensions are presented in Table 2. As shown in Table 2, the initial concentration of the dye in the range of 10–50 mg/L, the concentration of adsorbent in the range of 1–5 g/L, and the processing time in the range of 10–240 min were investigated.

Figure 4 presents the curves of Congo red dye removal percentage as a function of time at different concentrations of the SSPA. As shown in Figure 4, after 10 min, more than 57% of the dye in the aqueous solution was removed. However, with a further passage of time beyond 10 min, the Congo red uptake decreased over time, while the color removal percent still increased. At 120 min, the color removal percent had become almost constant over time, but still, the dye removal rate slightly increased until 180 min. Thus, the Congo red adsorption process on the adsorbent by changing the residence time can include two stages: rapid initial

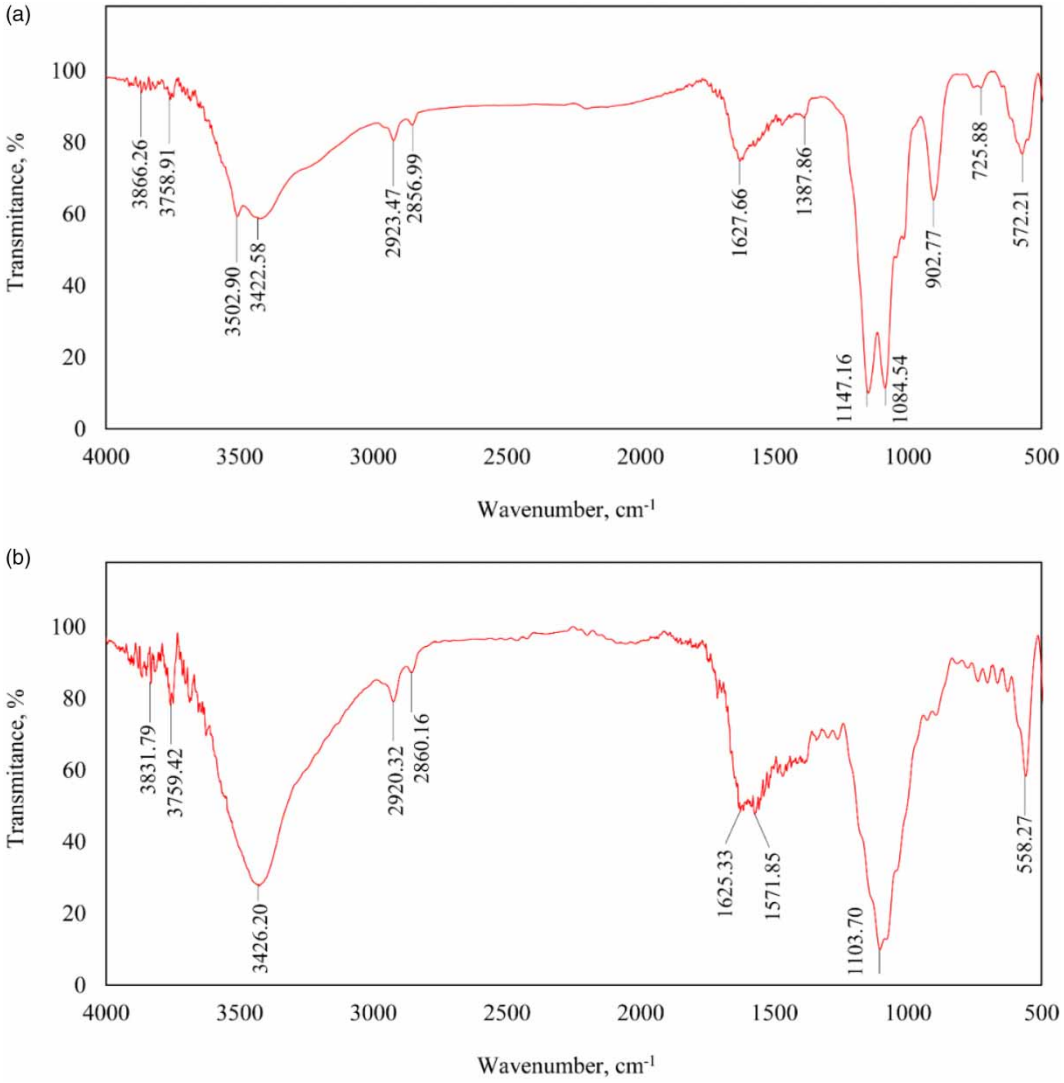

Figure 3 | FTIR spectrum of the SSPA; (a) before adsorption and (b) after adsorption.

Table 2 | Operational variables in Congo dye adsorption process and their levels

Factor	Symbol	Unit	Levels
Congo red initial concentration	C_i	mg/L	10, 30, 50
Adsorbent concentration	M	g/L	1, 3, 5
Time	t	min	10, 20, 30, 60, 90, 120, 150, 180, 240

adsorption and slow adsorption at the process end. It is clear that the initial rapid adsorption occurs due to the high affinity of Congo red and the adsorbent. Furthermore, the high adsorption sites and mass transfer gradient between the adsorbent and Congo red can be found among the explanations for this rapid adsorption. On the other hand, because the adsorption sites are saturated, which leads to a decrease in the vacancy numbers, the amount of adsorbent decreases at the last time (Nodehi *et al.* 2020).

As the diagrams in Figure 4 indicate, the adsorbent concentration plays an important role in the percentage of Congo red dye removal. With an increase in the adsorbent concentration from 1 to 3 g/L, a significant increase in Congo red dye removal percentage was observed. When increasing the adsorbent concentration from 3 to 5 g/L, the Congo red uptake decreased slightly and remained unchanged in some cases.

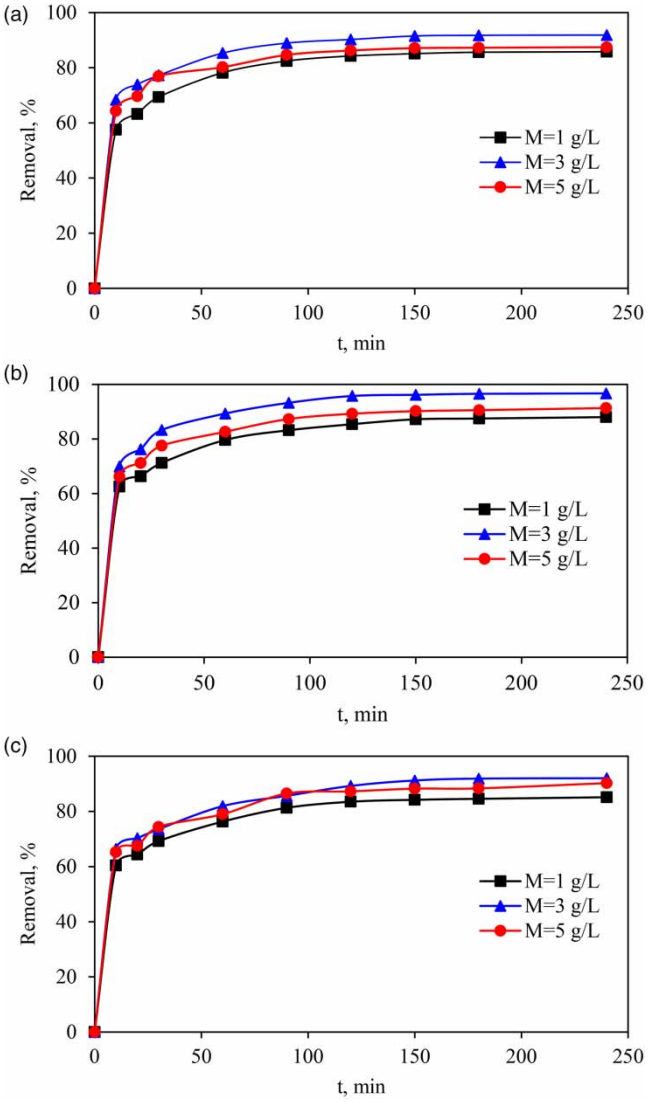

Figure 4 | Congo red dye removal diagrams over time at different concentrations of SSPA: (a) initial dye concentration of 10 mg/L, (b) initial dye concentration of 30 mg/L, and (c) initial dye concentration of 50 mg/L.

The diagrams in Figure 5 present the amount of Congo red adsorbed in grams of the adsorbent (q_t) over time. As shown in these figures, at low adsorbent concentrations ($M = 1$ g/L), the highest amount of adsorbed dye per gram of the adsorbent was observed, and with increasing the adsorbent concentration to 3 and then 5 g/L, the amount of adsorbed dye in grams reduced. In other words, the more adsorbents there are, the lower the ratio of adsorbed dye per gram of the adsorbent. Considering the diagrams in Figure 5, it is also worth noting that with increasing the adsorbent concentration, the time required to reach the final amount of adsorbed dye decreased due to more availability of adsorbent and the lower time of the adsorption process.

Considering the results presented in Figures 4 and 5, the dye concentration of 50 mg/L, the adsorbent concentration of 3 g/L, and the time of 180 min can be introduced as the optimal operating conditions. Under these conditions, the percentage of dye removal was 91.89% and the amount of dye adsorbed per gram of the adsorbent was 15.32 mg/g.

3.3. Kinetic modeling of Congo red adsorption on SSPA

In this work, two adsorption kinetic models were used, pseudo-first-order and pseudo-second-order to determine the boundary phase velocity and adsorption behavior (Samimi & Shahriari-Moghadam 2021). Primarily, a pseudo-first-order model is used to explore the adsorption processes (Piri & Sepehr 2022). The pseudo-first-order kinetic equation, also known as the Lagergren equation, assumes that the absorption rate of the adsorption

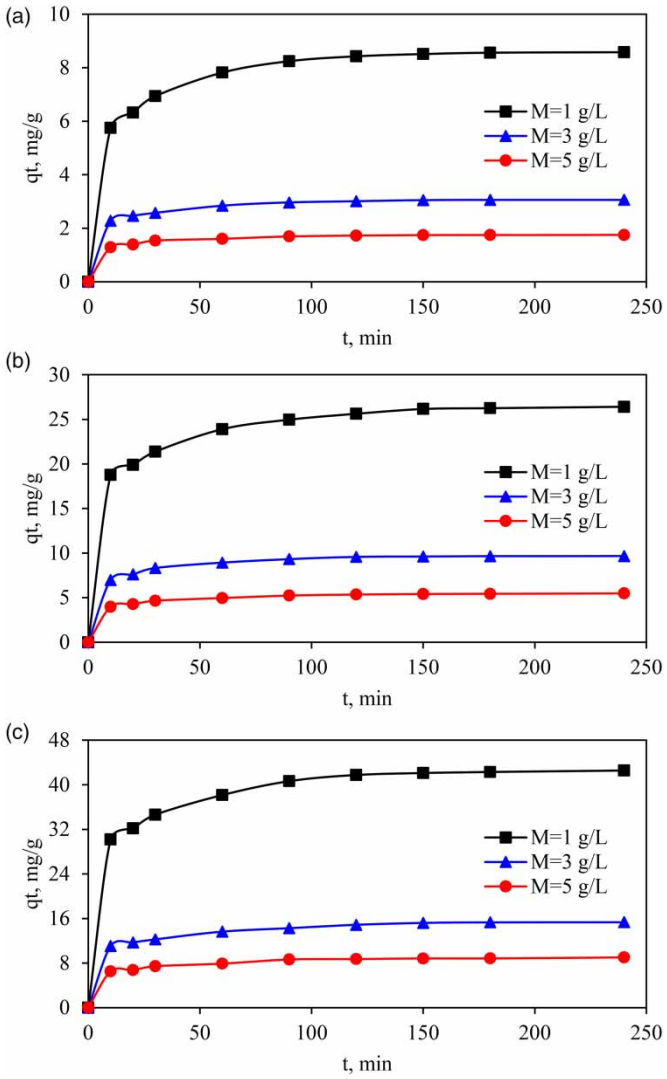

Figure 5 | Diagrams of the amount of Congo red dye adsorbed (adsorption capacity) over time at different concentrations of SSPA; (a) initial dye concentration of 10 mg/L, (b) initial dye concentration of 30 mg/L, and (c) initial dye concentration of 50 mg/L.

sites is proportional to the number of vacancies (Azimi *et al.* 2019). This term is represented as follows:

$$\frac{dq_t}{dt} = k_1(q_e - q_t) \xrightarrow{t=0,\ q_t=0} \ln(q_e - q_t) = \ln q_e + k_1 t \tag{3}$$

where q_t and q_e are the Congo red amount adsorbed at the residence time of t and equilibrium, respectively, and k_1 is the pseudo-first-order equation per min.

When the adsorption fits the first-order model, $\ln(q_e - q_t)$ versus t must represent a linear relationship, and the values of k_1 and q_e can be determined using the slope and the intercept (Samimi *et al.* 2023). Table 3 represents the values for q_e(exp.), q_e(calc.), k_1, and R^2 for the pseudo-first-order model. As shown in this table, despite the high correlation coefficient ($R^2 > 0.90$), the calculated q_e values deviate from the experimental q_e. Therefore, the adsorption process of Congo red cannot be described by a pseudo-first-order model.

Therefore, a pseudo-second-order model was used to determine the adsorption process. The second-order kinetics model is based on the assumption that the filling rates of the adsorbed sites are proportional to the square of the unoccupied sites (Samimi & Mansouri 2023). Furthermore, the number of occupied sites is directly proportional to the percentage of dye adsorbed, which is widely used in uptake processes (Özcan & Özcan

Table 3 | Results and parameters of pseudo-first-order and pseudo-second-order adsorption equations

		Pseudo-first-order			Pseudo-second-order		
C_i	q_e (exp)	q_e (calc)	k_1 (min^{-1})	R^2	q_e (calc)	k_2 ($g \cdot mg^{-1} \cdot min^{-1}$)	R^2
10	3.06	1.76	0.0353	0.9616	3.14	0.0603	0.9999
30	9.67	5.48	0.0339	0.9821	9.92	0.0187	0.9999
50	15.34	11.48	0.0334	0.9570	15.85	0.0084	0.9995

2005). This model is represented by the following equation:

$$\frac{dq_t}{dt} = k_2(q_e - q_t)^2 \xrightarrow{t=0,\ q_t=0} \frac{t}{q_t} = \frac{t}{q_e} + \frac{1}{k_2 q_e} \tag{4}$$

where q_t and q_e are the Congo red amount adsorbed at the residence times of t and equilibrium, respectively, and k_2 is the constant adsorption rate of the pseudo-second-order equation ($g \cdot mg^{-1}\ min^{-1}$).

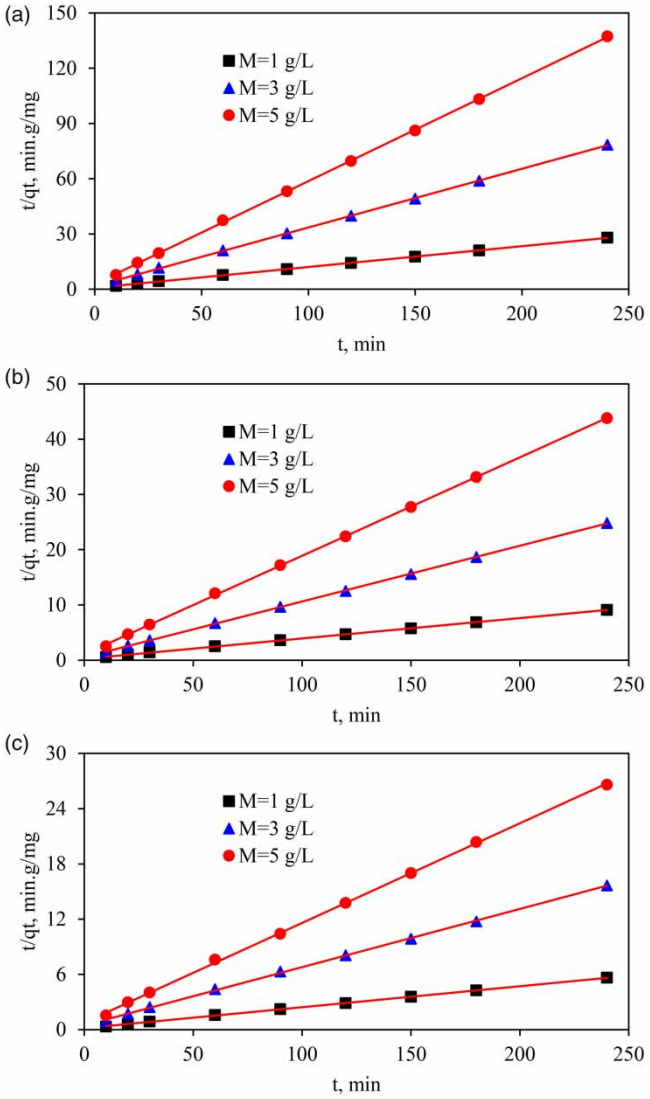

Figure 6 | Linear graphs of pseudo-second-order equations (t/q_t per t) at different concentrations of the SSPA; (a) initial dye concentration of 10 mg/L, (b) initial dye concentration of 30 mg/L, and (c) initial dye concentration of 50 mg/L.

According to Equation (4), when the t/q_t diagram per t has a linear relationship, the pseudo-second-order kinetic model is suitable for adsorbing the Congo red dye on the SSPA. Figure 6 shows that t/q_t has a significant linear relationship with t, which is proved by a high correlation coefficient ($R^2 \gg 0.99$). In addition, as seen in Table 3, the calculated q_e values correspond to the experimental ones. These results indicate a higher correlation of the pseudo-second-order equation than the first-order equation. Similar results on the Congo red adsorption have been observed in other works (Kumari *et al.* 2020; Li *et al.* 2020; Said *et al.* 2020; Extross *et al.* 2023; Vinayagam *et al.* 2023).

3.4. Adsorption reusability

The reusing process of the adsorbent was carried out according to the stated method under optimal conditions (initial dye concentration of 50 mg/L, residence time of 180 min and adsorbent concentration of 3 g/L). Different solvents were used to wash the adsorbent, and 1 M NaOH solution, 65% double-distilled water, and ethanol, respectively, had an acceptable performance in the washing process. Figure 7 summarizes the results of the washing process of SSPA. Based on the results presented in Figure 7, the use of one molar NaOH solution made it possible to wash the adsorbent for five rounds of reuse while retaining the Congo red dye removal capacity. Double-distilled water at 65 °C was able to wash the adsorbent well for four times. Finally, using ethanol, the adsorbent washing process was performed for three rounds while maintaining the Congo red dye removal capacity.

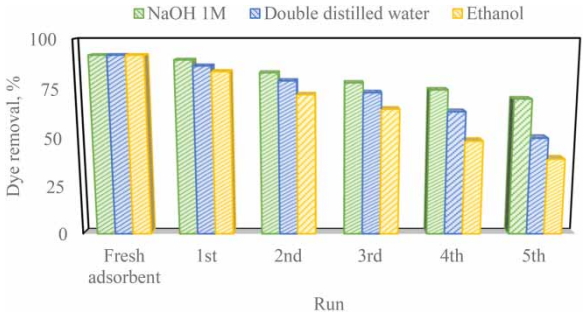

Figure 7 | Results of the washing process of the adsorbent used in this study by different solvents.

4. CONCLUSION

In general, most synthetic adsorbents, which can be used for dye removal from aquatic solutions are expensive and harmful to the environment. In this study, SSPA, a cheap and eco-friendly adsorbent, was prepared and used as an unusable waste to adsorb Congo red dye. The effect of initial dye concentration, SSPA concentration and process time on Congo red removal was evaluated. The results showed that the SSPA had a good adsorption capacity of Congo red dye. Moreover, in the present research, both pseudo-first-order and pseudo-second-order kinetic models were used for modeling, resulting in higher accuracy of the pseudo-second-order model ($R^2 \gg 0.99$). Finally, the washing process of the adsorbent used by different solvents was investigated, confirming the solution with one molar concentration had a high capacity to wash the adsorbent used in this work.

DATA AVAILABILITY STATEMENT

All relevant data are included in the paper or its Supplementary Information.

CONFLICT OF INTEREST

The authors declare there is no conflict.

REFERENCES

Abukhadra, M. R., Adlii, A. & Bakry, B. M. 2019 Green fabrication of bentonite/chitosan@cobalt oxide composite (BE/CH@Co) of enhanced adsorption and advanced oxidation removal of Congo red dye and Cr (VI) from water. *International Journal of Biological Macromolecules* **126**, 402–413.

Al-Zoubi, H., Zubair, M., Manzar, M. S., Manda, A. A., Blaisi, N. I., Qureshi, A. & Matani, A. 2020 Comparative adsorption of anionic dyes (eriochrome black t and Congo red) onto jojoba residues: Isotherm, kinetics and thermodynamic studies. *Arabian Journal for Science and Engineering* **45**, 7275–7287.

Azimi, N., Azimi, P., Samimi, M. & Jalilian, T. M. 2019 Ultrasonic-assisted adsorption of Ni (II) ions from aqueous solution onto Fe_3O_4 nanoparticles. *Advances in Nanochemistry* **1**(2), 66–72.

Bensalah, H., Younssi, S. A., Ouammou, M., Gurlo, A. & Bekheet, M. F. 2020 Azo dye adsorption on an industrial waste-transformed hydroxyapatite adsorbent: Kinetics, isotherms, mechanism and regeneration studies. *Journal of Environmental Chemical Engineering* **8**(3), 103807.

Bhat, S. A., Zafar, F., Mondal, A. H., Mirza, A. U., Haq, Q. M. R. & Nishat, N. 2020 Efficient removal of Congo red dye from aqueous solution by adsorbent films of polyvinyl alcohol/melamine-formaldehyde composite and bactericidal effects. *Journal of Cleaner Production* **255**, 120062.

Dai, H., Huang, Y., Zhang, H., Ma, L., Huang, H., Wu, J. & Zhang, Y. 2020 Direct fabrication of hierarchically processed pineapple peel hydrogels for efficient Congo red adsorption. *Carbohydrate Polymers* **230**, 115599.

Dbik, A., Bentahar, S., El Khomri, M., El Messaoudi, N. & Lacherai, A. 2020 Adsorption of Congo red dye from aqueous solutions using tunics of the corm of the saffron. *Materials Today: Proceedings* **22**, 134–139.

Drobyazko, S., Skrypnyk, M., Radionova, N., Hryhorevska, O. & Matiukha, M. 2021 Enterprise energy supply system design management based on renewable energy sources. *Global Journal of Environmental Science and Management* **7**(3), 369–382.

Ehzari, H., Safari, M., Samimi, M., Shamsipur, M. & Gholivand, M. B. 2022 A highly sensitive electrochemical biosensor for chlorpyrifos pesticide detection using the adsorbent nanomatrix contain the human serum albumin and the Pd: CdTe quantum dots. *Microchemical Journal* **179**, 107424.

Extross, A., Waknis, A., Tagad, C., Gedam, V. & Pathak, P. 2023 Adsorption of Congo red using carbon from leaves and stem of water hyacinth: Equilibrium, kinetics, thermodynamic studies. *International Journal of Environmental Science and Technology* **20**(2), 1607–1644.

Fawzy, M. A. & Gomaa, M. 2020 Use of algal biorefinery waste and waste office paper in the development of xerogels: A low cost and eco-friendly biosorbent for the effective removal of Congo red and Fe (II) from aqueous solutions. *Journal of Environmental Management* **262**, 110380.

Gupta, V. K., Agarwal, S., Ahmad, R., Mirza, A. & Mittal, J. 2020 Sequestration of toxic Congo red dye from aqueous solution using ecofriendly guar gum/activated carbon nanocomposite. *International Journal of Biological Macromolecules* **158**, 1310–1318.

Hamad, M. T. & Saied, M. S. 2021 Kinetic studies of Congo red dye adsorption by immobilized *Aspergillus niger* on alginate. *Applied Water Science* **11**, 1–12.

Han, R., Zhang, L., Song, C., Zhang, M., Zhu, H. & Zhang, L. 2010 Characterization of modified wheat straw, kinetic and equilibrium study about copper ion and methylene blue adsorption in batch mode. *Carbohydrate Polymers* **79**(4), 1140–1149.

Harja, M., Buema, G. & Bucur, D. 2022 Recent advances in removal of Congo Red dye by adsorption using an industrial waste. *Scientific Reports* **12**(1), 6087.

Jalali, M. & Aboulghazi, F. 2013 Sunflower stalk, an agricultural waste, as an adsorbent for the removal of lead and cadmium from aqueous solutions. *Journal of Material Cycles and Waste Management* **15**, 548–555.

Khan, R. R. M., Qamar, H., Hameed, A., Rehman, A. U., Pervaiz, M., Saeed, Z., Adnan, A. & Ch, A. R. 2022 Biological and photocatalytic degradation of Congo red, a diazo sulfonated substituted dye: A review. *Water, Air, & Soil Pollution* **233**(11), 468.

Kumari, R., Mohanta, J., Dey, B. & Dey, S. 2020 Eucalyptus leaf powder as an efficient scavenger for Congo red from water: Comprehensive batch and column investigation. *Separation Science and Technology* **55**(17), 3047–3059.

Lei, C., Zhu, X., Zhu, B., Yu, J. & Ho, W. 2016 Hierarchical NiO–SiO_2 composite hollow microspheres with enhanced adsorption affinity towards Congo red in water. *Journal of Colloid and Interface Science* **466**, 238–246.

Li, Z., Hanafy, H., Zhang, L., Sellaoui, L., Netto, M. S., Oliveira, M. L., Seliem, M. K., Dotto, G. L., Bonilla-Petriciolet, A. & Li, Q. 2020 Adsorption of Congo red and methylene blue dyes on an ashitaba waste and a walnut shell-based activated carbon from aqueous solutions: Experiments, characterization and physical interpretations. *Chemical Engineering Journal* **388**, 124263.

Liu, J., Wang, N., Zhang, H. & Baeyens, J. 2019 Adsorption of Congo red dye on $Fe_xCo_{3-}xO_4$ nanoparticles. *Journal of Environmental Management* **238**, 473–483.

Madan, S., Shaw, R., Tiwari, S. & Tiwari, S. K. 2019 Adsorption dynamics of Congo red dye removal using ZnO functionalized high silica zeolitic particles. *Applied Surface Science* **487**, 907–917.

Magdalane, C. M., Priyadharsini, G. M. A., Kaviyarasu, K., Jothi, A. I. & Simiyon, G. G. 2021 Synthesis and characterization of TiO_2 doped cobalt ferrite nanoparticles via microwave method: Investigation of photocatalytic performance of Congo red degradation dye. *Surfaces and Interfaces* **25**, 101296.

Mambwe, M., Kalebaila, K. & Johnson, T. 2021 Remediation technologies for oil contaminated soil. *Global Journal of Environmental Science and Management* **7**(3), 419–438.

Manjarrez Paba, G., Baldiris Ávila, R. & Baena Baldiris, D. 2021 Application of environmental bacteria as potential methods of azo dye degradation systems. *Global Journal of Environmental Science and Management* **7**(1), 131–154.

Moghadam, H. & Samimi, M. 2022 Effect of condenser geometrical feature on evacuated tube collector basin solar still performance: Productivity optimization using a Box-Behnken design model. *Desalination* **542**, 116092.

Mohammadi, M., Mohammadi Torkashvand, A., Biparva, P. & Esfandiari, M. 2021 The ability of layered double hydroxides for nitrate absorption and desorption in crop and fallow rotation. *Global Journal of Environmental Science and Management* **7**(1), 59–78.

Mohmmadkhani, S., Yeganeh, J. & Nazemi, S. 2016 Sunflower waste biomass as a remarkable adsorbent for removal of heavy metals from waste waters. *International Journal of Health Studies* **2**(3), 26–30.

Nimesha, S., Hewawasam, C., Jayasanka, D., Murakami, Y., Araki, N. & Maharjan, N. 2022 Effectiveness of natural coagulants in water and wastewater treatment. *Global Journal of Environmental Science and Management* **8**(1), 101–116.

Nodehi, R., Shayesteh, H. & Kelishami, A. R. 2020 Enhanced adsorption of Congo red using cationic surfactant functionalized zeolite particles. *Microchemical Journal* **153**, 104281.

Nuryadin, A. & Imai, T. 2021 Application of amorphous zirconium (hydr)oxide/MgFe layered double hydroxides composite in fixed-bed column for phosphate removal from water. *Global Journal of Environmental Science and Management* **7**(4), 485–502.

Oliver Paul Nayagam, J. & Prasanna, K. 2023 Response surface methodology and adaptive neuro-fuzzy inference system for adsorption of reactive orange 16 by hydrochar. *Global Journal of Environmental Science and Management* **9**(3), 373–388.

Özcan, A. & Özcan, A. S. 2005 Adsorption of Acid Red 57 from aqueous solutions onto surfactant-modified sepiolite. *Journal of Hazardous Materials* **125**(1–3), 252–259.

Piri, M. & Sepehr, E. 2022 Phosphorus recovery from domestic sewage sludge in the presence of waste grape pruning biochar. *Global Journal of Environmental Science and Management* **8**(4), 575–588.

Said, A. E.-A. A., Aly, A. A., Goda, M. N., Abd El-Aal, M. & Abdelazim, M. 2020 Adsorptive remediation of Congo Red Dye in aqueous solutions using acid pretreated sugarcane bagasse. *Journal of Polymers and the Environment* **28**, 1129–1137.

Samimi, M. 2024 Efficient biosorption of cadmium by *Eucalyptus globulus* fruit biomass using process parameters optimization. *Global Journal of Environmental Science and Management* **10**(1), 27–38.

Samimi, M. & Mansouri, E. 2023 Efficiency evaluation of *Falcaria vulgaris* biomass in Co (II) uptake from aquatic environments: Characteristics, kinetics and optimization of operational variables. *International Journal of Phytoremediation*, 1–11. https://doi.org/10.1080/15226514.2023.2250462.

Samimi, M. & Moeini, S. 2020 Optimization of the Ba^{+2} uptake in the formation process of hydrogels using central composite design: Kinetics and thermodynamic studies of malachite green removal by Ba-alginate particles. *Journal of Particle Science and Technology* **6**(2), 95–102.

Samimi, M. & Nouri, J. 2023 Optimized zinc uptake from the aquatic environment using biomass derived from *Lantana camara* L. stem. *Pollution* **9**(4), 1925–1934.

Samimi, M. & Safari, M. 2022 TMU-24 (Zn-based MOF) as an advance and recyclable adsorbent for the efficient removal of eosin B: Characterization, equilibrium, and thermodynamic studies. *Environmental Progress & Sustainable Energy* **41**(5), e13859.

Samimi, M. & Shahriari-Moghadam, M. 2021 Isolation and identification of *Delftia lacustris* Strain-MS3 as a novel and efficient adsorbent for lead biosorption: Kinetics and thermodynamic studies, optimization of operating variables. *Biochemical Engineering Journal* **173**, 108091.

Samimi, M. & Shahriari-Moghadam, M. 2023 The *Lantana camara* L. stem biomass as an inexpensive and efficient biosorbent for the adsorptive removal of malachite green from aquatic environments: Kinetics, equilibrium and thermodynamic studies. *International Journal of Phytoremediation* **25**(10), 1328–1336.

Samimi, M., Zakeri, M., Alobaid, F. & Aghel, B. 2023 A brief review of recent results in arsenic adsorption process from aquatic environments by metal-organic frameworks: Classification based on kinetics, isotherms and thermodynamics behaviors. *Nanomaterials* **13**(1), 60.

Siddiqui, S. I., Allehyani, E. S., Al-Harbi, S. A., Hasan, Z., Abomuti, M. A., Rajor, H. K. & Oh, S. 2023 Investigation of Congo Red toxicity towards different living organisms: A review. *Processes* **11**(3), 807. Available from: https://www.mdpi.com/2227–9717/11/3/807.

Thinakaran, N., Baskaralingam, P., Pulikesi, M., Panneerselvam, P. & Sivanesan, S. 2008 Removal of Acid Violet 17 from aqueous solutions by adsorption onto activated carbon prepared from sunflower seed hull. *Journal of Hazardous Materials* **151**(2–3), 316–322.

Uygunoz, D., Demir, F., Ozen, M. Y. & Derun, E. M. 2022 Sunflower waste–manganese iron oxide composite for hazardous dye removal. *Chemical Data Collections* **40**, 100893.

Vinayagam, R., Kandati, S., Murugesan, G., Goveas, L. C., Baliga, A., Pai, S., Varadavenkatesan, T., Kaviyarasu, K. & Selvaraj, R. 2023 Bioinspiration synthesis of hydroxyapatite nanoparticles using eggshells as a calcium source: Evaluation of Congo red dye adsorption potential. *Journal of Materials Research and Technology* **22**, 169–180.

Wekoye, J. N., Wanyonyi, W. C., Wangila, P. T. & Tonui, M. K. 2020 Kinetic and equilibrium studies of Congo red dye adsorption on cabbage waste powder. *Environmental Chemistry and Ecotoxicology* **2**, 24–31.

You, L., Huang, C., Lu, F., Wang, A., Liu, X. & Zhang, Q. 2018 Facile synthesis of high performance porous magnetic chitosan-polyethylenimine polymer composite for Congo red removal. *International Journal of Biological Macromolecules* **107**, 1620–1628.

Zhou, J., Lü, Q.-F. & Luo, J.-J. 2017 Efficient removal of organic dyes from aqueous solution by rapid adsorption onto polypyrrole–based composites. *Journal of Cleaner Production* **167**, 739–748.

Zong, E., Fan, R., Hua, H., Yang, J., Jiang, S., Dai, J., Liu, X. & Song, P. 2023 A magnetically recyclable lignin-based bio-adsorbent for efficient removal of Congo red from aqueous solution. *International Journal of Biological Macromolecules* **226**, 443–453.

First received 27 September 2023; accepted in revised form 27 November 2023. Available online 18 December 2023